Photovoltaic Canopies: Thermodynamics to Achieve a Sustainable Systems Approach to Mitigate the Urban Heat Island Hysteresis Lag Effect.

Jay S. Golden, Director

Sustainable Materials
and
Renewable Technologies Program

Arizona State University
Main Campus
P.O. Box 873211
Tempe, Arizona 85287-3211
Phone / Fax: +1-(480) 965-4951 / (480) 965-8087
Email: **jay.golden@asu.edu**

Abstract

At a time of greater attention to global climate change and increased costs of energy, our planet is rapidly urbanizing and transitioning regions from the natural rural vegetation to man-made urban engineered infrastructure. The anthropogenic-induced change has manifested itself in microscale and mesoscale increases in temperatures in comparison to adjacent rural regions which is known as the Urban Heat Island effect ΔT_{u-r} (Oke, 1987, Brazel, 2003) and results in the increased need electricity for mechanical cooling as well as various adverse environmental, social and economic consequences for local and global communities (Golden, 2004).

Prior research has documented between 29% to 45% of the urban fabric is comprised of paved surfaces to support mobility (Akbari et al. 1999). The increase of paved surfaces as a function of thermodynamics alters the urban energy budget due to changes in albedo, thermal mass as well as conduction, convection and evapotranspiration. An emerging engineering option to reduce the significant role that surface pavements play in adding to the urban heat island is to capitalize on the capturing and shading of incident solar energy by means of utilization of photovoltaic panels to provide covered parking for this large portion of the urban fabric.

Keywords: Multi-Junction Cells, Solar Energy, Hysteresis Lag, Pavements, Thermodynamics, Band Gap, Urban Heat Island, Photovoltaics, Sustainable Development. Total word count: 8,467 with references and figures.

”The total energy of the universe is constant. The total entropy of the universe strives to reach a maximum”

- Rudolf Clausius -

1. INTRODUCTION

The urban climate is influenced by terrain, anthropogenic heat, urban geometry, and substantially by the engineered materials which comprise pavements and the built environment. This research is focused on understanding the dynamics of photovoltaics can serve as an improved mitigation strategy for the adverse temporal influences of surface and parking pavements primarily realized in the urban heat island hysteresis lag effect as compared to the more conventional urban forestry option. Akbari et al. (1999) detailed that 39% of the area seen from above the urban canopy (tree canopy) consisted of paved surfaces including roads, parking areas and sidewalks. Similar evaluations of metropolitan areas of Salt Lake City, Utah, Sacramento, California and Chicago, Illinois revealed the percentage of paved areas ranged from 30% to 39% as seen above the canopy and 36% to 45% viewed under the canopy layer.

Low albedo hot mix asphalt (HMA) surfaces comprise approximately 80% of all paved surfaces of the urban fabric while concrete higher albedo materials represent the majority of the remainder of the 20% and are primarily utilized for high volume road networks. The materials and designs of these two types of paved surfaces vary as does convective turbulence as a function of vehicle traffic volume and speed. As

such, mitigative strategies and designs need to be developed accordingly to meet these varied surfaces.

The urban energy budget is represented by Brazel & Quatrocchi (2004) modified from Oke (1987) in which the energy budget is expressed in a simplified form as:

$$Q^* + Q_F = Q_E + Q_H + \Delta Qs + \Delta Qa \quad (1)$$

Where:

Q^* = net all-wave radiation

= K* + * (net short and long wave radiation)

Q_F = anthropogenic heat emission ($Q_{Fv} + Q_{FH} + Q_{FM}$)

Q_E = latent heat flux

Q_H = sensible heat flux

ΔQs = net heat storage in the city

ΔQa =net advection into or out of the city.

This research evaluated mitigation for surface pavements to reduce ΔQs and the hysteresis lag effect as presented in Figure #1.

<INSERT FIGURE #1>

A research regime was undertaken during the summer months of 2004 to evaluate two mitigation strategies for the hysteresis lag effect of surface parking pavements in the Phoenix, Arizona region. The 0.86^0F/decade warming rate for Phoenix is one of

the highest in the world for a population of its size and can be compared to other cities to highlight the effects of rapid urbanization in the region. For example, LA's rate was 0.8^0F/decade; SF, 0.2^0F/decade; Tucson, 0.6^0F/decade; Baltimore, 0.2^0F/decade; Washington, 0.5^0F/decade; Shanghai, 0.2^0F/decade; and Tokyo, 0.6^0F/decade (Hansen et al. 1999).

The first mitigation strategy examined was the utilization of urban forestry by which canopy coverage provides shading of paved surfaces. The second mitigation strategy evaluated was the utilization of engineered canopy covers including the utilization of photovoltaic solar panels as a possible sustainable engineering mitigation option. The research was undertaken to:

1. Quantify the diurnal surface and ambient temperature reductions with the utilization of urban forestry.
2. Quantify the diurnal pavement surface, canopy surface and ambient temperature reductions with the utilization of engineered parking canopies.
3. Evaluate the role of sky-view factor of urban forestry.
4. Evaluate the temporal impacts of utilizing photovoltaic panels as a mitigation strategy.
5. Introduce the sustainable systems associated with the development of photovoltaic canopies as a regional mitigation strategy to mitigate the urban heat island effect.

2. CONVENTIONAL URBAN FORESTRY

Increasing the amount of urban vegetation decreases local ambient air temperatures through shading and evapotranspiration. The U.S. Department of Agriculture Forest

Service (1999, 2000) estimates that maximum mid-day air temperature reductions are in the range of 0.07°F (-0.04°C) to 0.36°F (-0.2°C) for every one percent (+1%) increase in the canopy cover.

Shading can play an important role in the lower canopy boundary of parking lots by preventing solar radiation from coming in contact with, and being absorbed by, engineered materials. Incident solar radiation reaches a tree's canopy, with some percent utilized by the leaves for photosynthesis and with the remainder either reflected back into the atmosphere or transmitted to the engineered surface below. The latter quantity determines the tree's transmittance, which is typically 10% to 30% in the summertime. A mature 40 foot tree with a crown of 30 feet can decrease air temperature by transpiring as much as 40 gallons of water per day. Urban forestry canopy coverage over paved surfaces has been evaluated as a sustainable systems mitigation strategy for the Urban Heat Island effect by examining temporal, hydrocarbon and stormwater impacts while potentially increasing pavement longevity (Akbari et al. 1993; Asaeda et al. 1996; Scott et al. 1999; Xiao et al. 1998; McPherson et al. 1999). Some municipalities within the United States have adopted parking lot canopy coverage such as Sacramento, California which requires 50% canopy coverage of the total parking lot area within 15 years of a projects development (Sacramento City Ordinance 17.64.030).

To quantify the benefits of an urban forest canopy cover on engineered pavements, research was undertaken at the Arizona State University Research Park located approximately six miles to the south of the main campus in Tempe, Arizona. A typical urban parking lot was chosen at the ASU – US Army Flexible Display Center.

The pavements consisted of dense grade hot mix asphalt. The sampling location was void of any influence from urban geometry shading beyond that of near by urban forestry and the research area was made free from any anthropogenic heating sources. The total research area measured 100m x 100m with a centered 15m x 15m area monitored with the use of thermocouples. Temperatures were obtained within the hot mix asphalt parking surface just below grade on 4 sides of a cement low level planter box containing a South American mesquite (Figure #2), Argentine mesquite (Prosopis alba).

<INSERT FIGURE #2 HERE>

Ambient temperatures were also obtained on the trunk of the tree at 2m and a Campbell meteorological station was established adjacent to the research site measuring solar radiance, wind, rain and diurnal temperatures every 10 minutes.

The tree measured approximately 25 feet in height and had a trunk diameter of 5 feet and a canopy area of 20 feet diameter. The estimated instantaneous C assimilation flux values average around 10 umol/m2/s. The growth of this species depends on water availability and maintenance practices, but can reach height and spreads of 40' and 50' respectively but an average life span has not been established for Phoenix as the tree was introduced into the area less than 30 years ago. Variability includes poor planting location, wind throw, poor nursery stock, soil born pathogens, etc. In situ (the wilds of South American), the tree lives for hundreds of years. The cost of the tree in Phoenix for a typical 24” box is under $200 and variable depending on whether cutting or seed grown, whether it's a named cultivar or not.

2.1 Diurnal Findings

Sensors were arranged in within a four quadrant array (Figure #3) approximately 2m from the trunk of the tree in each navigational direction (north, south, east and west).

<INSERT FIGURE 3 HERE>

Each thermocouple sensor was covered by the canopy coverage of the tree. A control thermocouple as placed in the same HMA paving material approximately 30 meters to the south of the research canopy in an area fully exposed to solar influences (180° Ψ_{sky}). Additionally, the fully exposed sensor was free from any urban geometry or urban forestry influences.

2.2 Sky View Factor

Sky-view factor (Ψ_{sky}) is a dimensionless parameterization of the quantity of visible sky at a location which is represented between zero and one. Ψ_{sky} will approach unity in a perfectly flat and open terrain, unlike the urban region with various geometries of the built environment that reduce Ψ_{sky} (Chapman et al. 2001; Oke, 1992). In the urban region, Ψ_{sky} and 1- Ψ_{sky} give a measure of how much radiation will penetrate the canopy and how much will be intercepted by the canopy. Ψ_{sky} is determined for a specific point in space, i.e., it gives a measure of the open view to the sky to radiative transport relative to a specific location with a range of zero to one. Zero means that the sky is completely obstructed by canopy coverage or other geometry and all outgoing longwave radiation (L↑) would be intercepted by the obstacles. A rating of

one (1) indicates that the sky view is free of all obstacles and outgoing radiation would radiate freely to the sky (Brown and Grimmond, 2001). The hysteresis lag effect is impacted by Ψ_{sky} due to the limiting longwave radiation (L↑) by a canopy trapping effect.

Solar irradiance is impacted by altitude which is the angle up from the horizon. Zero degrees altitude means exactly on your local horizon, and 90 degrees is "straight up". Azimuth is the angle along the horizon, with zero degrees corresponding to North, and increasing in a clockwise fashion. Thus, 90 degrees is East, 180 degrees is South, and 270 degrees is West. Using these two angles, one can describe the apparent position of an object (such as the Sun at a given time).

The altitude and azimuth values are for the center of the apparent disk of the Sun. The altitude values include the effect of standard atmospheric refraction when the object is above the horizon. The azimuth values are computed with respect to true north (not magnetic). Azimuth (vertical angle) determinations around the compass of the vertical angle from the local flat surface to the tree overhang of the canopy for every 20 degrees of azimuth direction was obtained as was the sun's azimuth/angle position in the sky for each hour on the dates of the measurements of surface temperature. As presented in Figure #4 & #5, the azimuth and altitude angles were estimated from the flat horizon to edge of tree obstruction document where the sun passed within the tree canopy perimeter in its path through the sky horizon.

<INSERT FIGURE #4 HERE>

<INSERT FIGURE #5 HERE>

Field evaluations were conducted of the control site for which the diurnal timing shows up well in the surface temperature responses. Altitude and azimuth combine with the sky view factor to play a role in the ability of a thermal pocket such as the pavements being evaluated to be impacted by solar irradiance.

Data from the month of June 2004 was utilized as it is highly representative of the calm, clear diurnal cycles consistent with the most pronounced month of the urban heat island effect. The results of the research shows:

1. The fully exposed non-shaded HMA pavement maintained the highest surface temperature during the complete diurnal cycle with exception of the first cycle heating which occurs 0800-1200 hours when pavements on the eastern side of the tree canopy ran consistent with the fully exposed pavement. *(note: slight variations of surface pavements can be attributed to the installation of each thermocouple and patching of the pavement after installation of the thermocouples).*
2. The eastern, western and southern surface temperatures increased both as a function of solar radiance and solar altitude during the daytime.
3. Fully exposed surfaces had a higher rate of temperature increase, yet canopy coverage did not significantly reduce the rate of cooling of pavements under a tree versus fully exposed surface pavements.

<INSERT FIGURE #6 HERE>

Of consideration in parking areas is the role of human comfort. This was examined by evaluating ambient air temperatures at 2m height levels. The benefits of the canopy effect are present during highest solar radiance when the shaded canopy provided a -3.5° C benefit.

However, unlike pavement surface temperatures which retained a higher diurnal cycle temperature as a function of the hysteresis lag effect, upon sunset, ambient temperatures directly under the canopy coverage were higher on average by 1°C than fully exposed ambient temperatures. This held consistent until surface heating in the early morning hours (~0830 hours) as presented in Figure #7. The canopy effect of longwave radiation can help explain the lower cooling rate than a similarly sampled area with $180°\Psi_{sky}$.

<INSERT FIGURE #7 HERE>

3. AN ALTERNATIVE SUSTAINABLE ENERGY MITIGATION STRATEGY

This phase of research was carried out at the City of Phoenix, Arizona-Pecos Road Park and Ride Facility. The facility is utilized by residents of the Southeastern portion of the City to park their personal vehicles and utilize public transportation for areas of central city and throughout the region.

As seen in Figure #8, the facility which opened in 2003 accommodates 562-personal vehicles with covered canopy parking. The Salt River Project (SRP), a regional public utility joined with the city of Phoenix Transit Department in a $1 million

project to install solar power panels on covered parking structures on top of two existing sheet metal parking covers. The system is a fixed tilt flat system containing 768 modules of 165W each on two parking canopies. The array area for the combined parking system is 11,000 ft^2 which provides coverage for ~80 American sized vehicles.

<INSERT FIGURE #8 HERE>

The main PV power system has a design rating of 127kW dc or 100kW ac which will produce an annual output of ~ 178,000 kWh, enough to provide power to ~100 homes annually in the utility service area (SRP, 2003).

3.1 Micro-Climate Variability

During the month of June 2004, research was conducted utilizing hand-held Infrared Thermography, in-situ thermocouples and the establishment of a stationed meteorological station. Thermocouple sensors consist of two dissimilar metals, joined together at one end, which produce a small voltage at given temperatures. This voltage is measured and interpreted by a thermocouple thermometer. Self contained sensors that contain a battery, clock, temperature sensor and memory by Command Center™ which have a sensor accuracy of ±1°C and a range of -10° to 85°C were used. Each sensor can store 2,048 readings and can be set to sample at adjusted intervals by easy to use computer software. Each sensor is 1/4" x 3/4" in diameter with cable length typically of 12'. The sensors were programmed to obtain readings at twenty minute intervals.

One set of thermocouples was placed imbedded within the HMA pavement surface fully exposed with $180°\Psi_{sky}$. Additionally a second thermocouple was attached to a vertical stake at 2m height above ground surface (ags). A second set of thermocouples was placed at a "conventional" parking canopy area. This included placement within the HMA pavement, at 2m ags, directly underneath the canopy top and one just above the canopy top. A third set of thermocouples was placed at a modified photovoltaic parking canopy cover.

Similar to the conventional canopy, thermocouples were placed within the HMA pavement, at 2m ags, directly underneath the canopy top and one placed in the layer between the conventional canopy top and the bottom of the photovoltaic panels. The PV panels were approximately 4cm above the conventional panel. No thermocouple was placed at the top of the PV panels as the readings would present the incident solar absorption of the thermocouple and not the PV panel. The diurnal evaluations of the PV panel temperature is most appropriately evaluated at the base of PV panels.

3.2 Surface Temperature Evaluations

Understanding the diurnal temperature variability of the pavement surfaces serves as a first order indication of the ability to modify the hysteresis lag effect. The temperature variability for the three locations as represented on 14 June 2004 indicate that the fully exposed pavement receives and stores the greatest amount of energy reaching maximum surface temperatures of 65.5°C (149.9°F) while the pavement surfaces covered by the PV-conventional canopy tandem alignment reached the lowest maximum surface temperature of 38.5°C (101.3°F).

$$ÐΔT_{Exposed} = {}^{surface}T_{Max}\,(65.5°C) - {}^{surface}T_{Min}\,(28.5°C) = 37°C \quad (2)$$

$$ÐΔT_{Conv.\ Canopy} = {}^{surface}T_{Max}\,(39.5°C) - {}^{surface}T_{Min}\,(27.5°C) = 11°C \quad (3)$$

$$ÐΔT_{PV\ Modified\ Canopy} = {}^{surface}T_{Max}\,(38.5°C) - {}^{surface}T_{Min}\,(28.0°C) = 10.5°C \quad (4)$$

Where: ÐΔT = diurnal surface temperature delta

The thermographic evaluations provide a visualization of the surface temperature variability.

3.3 Canopy Top Variability

The examination of photovoltaics as a mitigation tool for the urban heat island has seen only limited research to date. Genchi et al. (2003) modeled large scale use of PV panels in a large area of Tokyo. The research was focused on building roof tops. They concluded the large-scale impact would be negligible but that energy consumption for cooling may be reduced by up to 10% by the shading effect. This research was interested in comparing the surface temperatures of the PV / canopy top versus the surface temperatures of the exposed pavements and the nocturnal energy storage and release. The urban heat island in many regions, including the greater Phoenix, Arizona region is primarily a nocturnal event.

By reducing heat storage (Q_s) there is the potential to mitigate the UHI at the micro and meso scales. Diurnal analysis indicated that the HMA typical parking lot surface maintained the highest surface temperatures throughout the diurnal cycle. The sheet metal conventional parking canopy top heated more rapidly than the photovoltaic

panels in pre-noon (1200 hours) where the PV panels then warmed up higher than the sheet metal canopy. The HMA pavement had the greatest rate of temperature increase of all three materials.

While post sundown and the influence of solar radiance the Photovoltaic panels had the fastest rate of temperature decrease. The hysteresis lag of the surface pavements Q_s is evident in the slow rate of cooling (Figure #9).

<INSERT FIGURE #9 HERE>

3.4 Variability Influences

Wind speed during the 24 hour period of 14 June 2004 obtained from the adjacent meteorological station averaged .86m/s with a high wind speed of 2.65 m/s sustained for less than 15 minutes around 1415 hours. Solar irradiance initiated at 0515 hours with the last recorded reading taken at 2000 hours. Maximum ambient air temperature of 40.98°C (105.76°F).

This particular facility is utilized by commuters who arrive prior to 0700 hours and leave their vehicle in place until post work (1700-1900 hours). No quantification of the anthropogenic heat flux was measured as a result of the vehicle engines. However, the flux is primarily generated during cool early morning hours for durations of less than one-hour which would be negligible to the diurnal hysteresis lag effect. The post work heat flux from vehicles is also minimized as vehicles are started and removed quickly from the parking area. A higher volume parking lot such as

those found in retail establishments would present higher fluxes primarily during peak shopping hours.

4.0 URBAN FORESTRY v. PHOTOVOLTAIC CANOPY MITIGATION

A comparative analysis was conducted to understand the mitigation dynamics of paved parking lot surface temperatures with an Urban Forestry canopy cover as compared to the same surface material covered by a photovoltaic canopy coverage. The evaluation period was for the diurnal cycle of 14 June 2004. The tree canopy coverage area

Meteorological and engineered pavement data was utilized for the same date of 14 June 2004. The Arizona State University Research Park (Urban Forestry canopy coverage) and the City of Phoenix Park and Ride lot (photovoltaic canopy coverage) are approximately 7.2 miles in distance by road networks. Of interest was comparing the $ÐΔT^{surface}$ achieved by both mitigation strategies. The resultant as presented in Figure # 10, the HMA surface shaded by a PV canopy achieves a -55.8°F reduction in comparison to the fully exposed HMA while the HMA surface mitigated by the urban forestry achieves a maximum reduction of -43.2°F.

The maximum temperature reduction for the urban forestry canopy would have been even lower if surface temperatures for the eastern shaded pavements were used as this area had greater rate of heating. In part this variation of surface temperature reductions between the two mitigation strategies can be explained due to the increased

sky view factor (Ψ_s) of the urban forestry mitigation strategy during the influence of solar irradiation. However, both covered HMA surfaces reach equilibrium at near sunset thus undermining the positive influence of the urban forestry Ψ_s.

<INSERT FIGURE #10 HERE>

Ambient air temperatures between both covered HMA surfaces in comparison to their adjacent fully exposed ambient air temperatures, both at 2m ags were obtained for the same time period.

4.1 Utilizing the Laws of Thermodynamics to Benefit Urban Climate

Unlike a dry paved surface which primarily absorbs, stores and re-radiates solar gains as long-wave radiation, a photovoltaic solar cell is a thermodynamic engine working between two heat reservoirs T_1 and T_2:

The explanation is observed as

T_1 - high temperature = the temperature of the Sun = 5762 K and

T_2 - low temperature = the temperature of the Earth = 288 K.

Its electric current consists of two parts: the light current, strongly dependent on T_1, and the dark current, strongly dependent both on T_2 and on material constants and technology parameters. (De Vos A., 1992). The rules of thermodynamics state:

The first law of Thermodynamics:

$$\Delta U = Q\text{-}W \tag{5}$$

Where: ΔU is the change in internal energy, Q is the heat added to the system and W is the work done by the system.

The second law of Thermodynamics, entropy. It is not possible for heat to flow from a colder body to a warmer body without any work having been done to accomplish this flow. Energy will not flow spontaneously from a low temperature object to a higher temperature object.

The efficiencies of systems is a key component in energy utilization. This runs counter to current philosophies of urban heat island mitigation which espouse utilization of high albedo engineered components to reduce solar gains. However, one of the primary goals in solar cell manufacturing is to reduce the reflective losses at specific wavelengths. The monocrystalline and polycrystalline silicon solar modules represent more than 80% of all the PV production market and they are highly reliable. In these technologies, the reflective losses are reduced from about 30% to about 6% by using surface coating, called anti-reflective coating, of the solar cells. By adjusting the thickness and material properties of these coatings and increasing albedo the light-to-electrical efficiency may be reduced. Thin film technologies such as amorphous silicon, Cadmium Telluride (CdTe) and Copper Indium Diselenide (CIS) represent less than 20% of the market. The efficiency of amorphous silicon is considerably lower (6-8%) than any other PV technologies. The CIS and CdTe are emerging technologies and are being evaluated and demonstrated for their reliability. The material and processing properties including band gap dictate the amount of reflected light. Visually, CdTe has the lowest albedo, CIS next highest albedo and Si with the highest albeo and a somewhat brown color.

4.2 Solar Radiation Balance – Excess Heat or Energy Generator

The sun emits almost all of its energy in a range of wavelengths from about $2x10^{-7}$ to $4x10^{-6}$ meters. Most of this energy is in the visible light region. Each wavelength corresponds to a frequency and energy: the shorter the wavelength, the higher the frequency and the greater the energy, which is expressed in electron-volts, (or eV). Red light is at the low-energy end of the visible spectrum and violet light is at the high-energy end, where it has half again as much energy as red light. In the invisible portions of the spectrum, radiation in the ultraviolet region (UV), which can burn the skin, has more energy than that in the visible region.

The sun is continually releasing an enormous amount of radiant energy into the solar system (QI). The Earth receives a tiny fraction of this energy; yet, an average of 1367 watts (W) reaches each square meter (m^2) of the outer edge of the Earth's atmosphere. The atmosphere absorbs and reflects some of this radiation (QR), including most X-rays and ultraviolet rays. Still, the amount of the sun's energy that reaches the surface of the Earth every hour is greater than the total amount of energy that the world's human population uses in a year.

<INSERT FIGURE #11 HERE>

Solar energy loss depends on the thickness of the atmosphere that the sun's energy must pass through. The radiation that reaches sea level at high noon in a clear sky is 1000 W/m^2 and is described as "air mass 1" (or AM1) radiation. As the sun moves lower in the sky, the light passes through a greater thickness (or longer path) of air,

losing more energy. Because the sun is overhead for only a short time, the air mass is normally greater than one—that is, the available energy is less than 1000 W/m^2.

The standard spectrum outside the Earth's atmosphere is called AM0, with no light passing through the atmosphere. AM0 is typically used to predict the expected performance of PV cells in space. The intensity of AM1.5D radiation is approximated by reducing the AM0 spectrum by 28%, where 18% is absorbed and 10% is scattered. The global spectrum is 10% greater than the direct spectrum. These calculations give about 970 W/m^2 for AM1.5G. However, the standard AM1.5G spectrum is "normalized" to give 1000 W/m^2, because of inherent variations in incident solar radiation. Flat panel collectors can utilize both diffuse and direct light while solar concentrating units can only utilize direct light.

AM1.5G (where G stands for "global" and includes both direct and diffuse radiation) or AM1.5D (which includes direct radiation only). The number "1.5" indicates that the length of the path of light through the atmosphere is 1.5 times that of the shorter path when the sun is directly overhead.

<INSERT FIGURE 12 HERE>

Solar cells respond differently to the different wavelengths, or colors, of light (Figure #12). For example, crystalline silicon can use the entire visible spectrum, plus some part of the infrared spectrum. But energy in part of the infrared spectrum, as well as longer-wavelength radiation, is too low to produce current flow (Figure #13). Higher-energy radiation can produce current flow, but much of this energy is likewise not

usable. In summary, light that is too high or low in energy is not usable by a cell to produce electricity as it simply transforms into heat.

<INSERT FIGURE 13 HERE>

5.0 BANDGAP OF ENERGIES

The first silicon solar cells developed in the 1950s by researchers at Bell Laboratories were not highly efficient but provided enough power to support electric appliances. At first, the devices were used primarily by toy manufacturers to make solar-powered miniature ships, radios, and other playthings.

Efficiency has been one of the reasons for the lack of greater utilization of photovoltaics as a primary energy generation source. Efficiency is closely tied to the engineered bandgap designs and capabilities. Bandgap energy is the amount of energy required to dislodge an electron from its covalent bond and allow it to become part of an electrical circuit. Vital to obtaining an efficient PV cell is to convert as much sunlight as possible into electricity. Therefore, to free an electron, the energy of a photon must be at least as great as the bandgap energy. However, photons with more energy than the bandgap energy will expend that extra amount as heat when freeing electrons. So, it's important for a PV cell to be "tuned"—through slight modifications to the silicon's molecular structure-to optimize the photon energy. Charge cannot flow in either a completely full or a completely empty band, but doping a semiconductor provides extra electrons or positively charged "holes" that can carry a current. Photons with just the right energy-the color of light that matches the bandgap-create electron-hole pairs and let current flow across the junction between positively

and negatively doped layers. Photons with too much energy are absorbed, but since each creates just one electron-hole pair, the excess energy is wasted as heat.

Crystalline silicon has a bandgap energy of 1.1 electron-volts (eV). (An electron-volt is equal to the energy gained by an electron when it passes through a potential of 1 volt in a vacuum.) The bandgap energies of other effective PV semiconductors range from 1.0 to 1.6 eV. In this range, electrons can be freed without creating extra heat. The photon energy of light varies according to the different wavelengths of the light. The entire spectrum of sunlight, from infrared to ultraviolet, covers a range of about 0.5 eV to about 2.9 eV. For example, red light has energy of about 1.7 eV, and blue light has an energy of about 2.7 eV.

Traditionally, most PV cells cannot use about 55% of the energy of sunlight, because this energy is either below the bandgap of the material or carries excess energy.

Different PV materials have different energy band gaps. Photons with energy equal to the band gap energy are absorbed to create free electrons. Photons with less energy than the band gap energy pass through the material.

The photoelectric effect is the basic physical process by which a PV cell converts sunlight into electricity. When light shines on a PV cell, it may be reflected, absorbed, or pass right through. But only the absorbed light generates electricity as electrons escape from their normal positions and become part of the electrical flow (current) in an electrical circuit. The built in electrical field of the PV cell provides the voltage to drive the current. This is accomplished by placing an "n-type" semiconductor with an abundance of electrons, which have a negative electrical charge with a different layer

of "p-type" semiconductor with an abundance of "holes," which have a positive electrical charge. Sandwiching these together creates a p/n junction at their interface, thereby creating an electric field. When n- and p-type silicon come into contact, excess electrons move from the n-type side to the p-type side. The result is a buildup of positive charge along the n-type side of the interface and a buildup of negative charge along the p-type side. The electrical field causes the electrons to move from the semiconductor toward the negative surface, where they become available to the electrical circuit. At the same time, the holes move in the opposite direction, toward the positive surface, where they await incoming electrons.

As an example using a Cadmium Telluride **(**CdTe) photovoltaic system, low energy light (infrared <1.44 eV) is not useful for generating electricity but it can create heat which will impact efficiency. An ideal photovoltaic cell in use for urban heat island mitigation would be designed to either maximize all available solar energy or reflect unused spectrums to allow for PV modules to be cooler and operate at a higher efficiency while promoting a reduced urban heat island effect. Solar incidence of exactly the bandgap (1.44 eV for CdTe) when absorbed by CdTe creates an electron-hole pair that can be used to produce useful electricity. Higher energy light such as UV to visible >1.44 eV generates electron-holes pairs but also generates heat. Thus, roughly one third of the available solar radiation is too low of energy, one third is converted to excess heat and one third can in principle be converted to electricity. As not all of the photogenerated electrons can be collected and as collected electrons do

not have all of their initial voltage, theoretical conversion efficiencies are less than 33%, e.g for CdTe the number is 28%.[1]

Thus the ideal module would absorb all radiation above the bandgap (energy > 1.44 eV) or about 2/3rd of the sun's power and it would be visually black. Ideally the module would also be an efficient IR reflector on the sunny side and an efficient IR radiator on the back side (in order to keep the module cool). Additional cooling benefits can be realized through convection (e.g. wind) and conduction.

5.1 Multijunction Cells – More Effective UHI Mitigation

A designed stop-gap method to maximize available energy is to use multiple different cells, with more than one band gap and more than one junction, to generate a voltage – Multijunction cells (also called "cascade" or "tandem" cells). Multijunction devices can achieve a higher total conversion efficiency because they can convert more of the energy spectrum of light to electricity. Researchers and engineers have developed multijunction cells which are stacked as individual single-junction cells in descending order of band gap.. The top cell captures the high-energy photons and passes the rest of the photons on to be absorbed by lower-band-gap cells. The most abundant volume of work has been in regards to gallium arsenide as one (or all) of the component cells. Such cells have reached efficiencies of around 35% under concentrated sunlight which is what would be required on a parking canopy design. Other materials studied for multijunction devices have been amorphous silicon and copper indium diselenide.

[1] Developed from conversations with Dr. Govindasamy Tamizhmani of the Photovoltaic Testing Laboratory and with Dr. Peter Meyers, Chief Scientists for First Solar Inc.

This stacking of materials of dissimilar band gaps makes it possible to broaden the range of wavelengths absorbed by a semiconductor and boost the efficiency of a solar cell above 35%. However, many times compounds of dissimilar materials, for example, Si (1.1-eV band gap) and AlGaAs (1.7 eV), often resist being stacked because of differences in their lattice parameters.

However, recent research by Yu et al. (2003) had identified that Indium nitride (InN) has a very low band gap--around 0.7 eV which had been thought to be 2 eV. Indium nitride can be alloyed relatively easily with GaN (3.4-eV band gap), and alloys of various compositions of indium, gallium, and nitrogen can be stacked readily to form multilayer (multijunction) materials thus engineers can develop new cells to cover the entire spectrum (Jacoby, 2004) a more efficient means to convert solar irradiance that theoretically can achieve power conversion efficiencies surpassing 50% (Yu et al. 2003) rather than relying of partial solar reflection or non-used thermal storage (hysteresis lag). To date, the most efficient cells are two-junction cells with about 30 percent efficiency.

Researchers at Lawrence Berkeley National Laboratories are investigating the potential for a multi-gap material which would be a single semiconductor with multiple band gaps. Indium gallium nitride solar cells could be made with more than two layers, perhaps a great many layers with only small differences in their bandgaps, for solar cells approaching the maximum theoretical efficiencies of better than 70 percent. It remains to be seen if a p-type version of indium gallium nitride suitable for solar cells can be made as parameters remain to be settled, like how far charge carriers can travel in the material before being reabsorbed.

6.0 SUSTAINABLE SYSTEM CONSIDERATIONS

6.1 Viability of Urban Forestry in Semi-Tropical Arid Regions

Urban forestry has been examined as a means to reduce the hysteresis lag and has been shown to be effective. However, the mitigation proposal requires an understanding of inter-related influences. One such influence is the urban climate itself. As presented in Figure 14, Baker et al. (2004) examined the changing dynamics of days cold stress vs. days heat stress from 1945 to 2003. Cold stress days as indicated by the white diamond have significantly reduced while heat stress days (those above 40°C) have increased. The broad and narrow leaf woody trees and shrubs used are generally grouped under the category of urban forestry in the Phoenix region. According to Baker et al. (2004) these species when exposed to supraoptimal, sublethal temperatures above 40C experience the most negative impact on photosynthesis (Farrar and Williams, 1991). Supraoptimal temperatures inhibit photosynthesis by decreasing the efficiency of photosynthetic enzymes (Huxman *et al*., 1998; Rokka *et al*., 2000; Crafts-Brandner and Salvucci, 2000) and increasing photorespiration (Law and Crafts-Brandner, 1999; Jordon and Orgen, 1984). Supraoptimal temperatures also increase growth and maintenance respiratory costs (Van Iersel and Linstrom, 1999), lower water-use efficiency (Martin *et al*., 1995), and the lower ET cooling potential of urban vegetation by stomatal inhibition of leaf transpirational water loss (Martin and Stabler, 2002). Because many of the

horticulture utilized in the region has been recently introduced, similar to the population, these plants are not adapted to the regional climatics and the stress of the increased heating days reduces evapotranspiration (Baker et al. 2004).

Celestian and Martin (2003) studied effects of parking lot location on size and physiology of four regionally common landscape tree species in the Phoenix region over a two year period. Parking lot trees must contend with a number of micro-environmental stresses that might adversely affect their growth. In addition to restricted rooting volumes and limited access to water and nutrients, some parking lot trees are exposed to elevated rhizosphere and canopy air temperatures caused by intense sunlight and the absorptive and reradiant properties of asphalt and concrete surface covers (Kjelgren and Montague, 1998). Continuous exposure of trees, especially those within parking lot landscaped medians, to these conditions might adversely impact tree performance by either direct injury of tissues or by indirect inhibition of physiological processes like nitrogen and carbon assimilation. In their study, Celestian and Martin (2003) examined four common tree species; (1) *Brachychiton populneus,* (bottle tree), (2) *Fraxinus velutina* Torr. (Arizona ash), (3) *Prosopis alba* Griebach (South American mesquite), and (3) *Ulmus parvifolia* Jacq. (Chinese elm). Bottle trees were located at two parking lots, Arizona ash at three parking lots, South American mesquite at three parking lots, and Chinese elm at four parking lots. At each parking lot, the researchers collected samples of rhizosphere soil [15 to 30 cm (6 to 12 in) depth] from under the canopy drip line at both the median and perimeter locations for analysis of soil chemical properties. Their research revealed trees located within the landscaped medians were smaller than those

within the landscaped areas along the parking lot perimeter, though the extent and significance of this difference was species specific. The findings also supported prior research that showed that elevated root zone temperatures similar to those that can occur in soil in the vicinity of parking lot landscaped medians can inhibit leaf photosynthesis and conductance of trees (Martin et al., 1995; Celestian and Martin, 2003). Additionally as presented in Figure # 14, the Urban Heat Island effect as represented in the Phoenix, Arizona region has caused an increase in the re-occurring heat stress days which can reduce the potential effectiveness of an urban forestry mitigation strategy.

<INSERT FIGURE #14 HERE>

6.2 Water Resources – The Sustainable Energy Equation

Because of the increased stress, plant viability will require an additional consumption rate of municipal water to initiate and maintain a meso-sclae urban forestry mitigation strategy.

In the United States, thermoelectric power generation withdrawals more water than any other form of water usage (Figure #15) including agricultural irrigation or municipal water consumption. Water use in the United States (USGS, 2004). As measured by freshwater withdrawals in 1985, averaged 15 million m^3/s (338 billion gal/day) (Carr et al. 1990). Four million m^3/s (ninety-two billion gal/day), or 27 percent of the water withdrawn, was consumed (e.g., by evaporation) and thus was not directly returned to the body of water.

<INSERT FIGURE # 15 HERE>

The primary use of water at power plants is for condensing steam, i.e., cooling steam back to water. Water is also used to make up the high-pressure steam for rotating turbines to generate electricity (Energy Foundation, 2003).

Water balance as a function of energy production has been estimated from 2.54 litres (0.67 gallons) of water per kWh produced via a coal-fired power plant while a natural-gas fired combined cycle power plant consumes 1.25 litres (0.33 gallons) of waters per kWh produced (SWEEP 2002). The National Energy Technology Laboratory operated by the United States Department of Energy estimates up to 94.64 litres (25 gallons) of water is required to produce 1kWh of electricity from a coal plant (NETL, 2004).

A 1996 Industrial Water Survey and report (Sharff et al. 2002) gathered information on the volume of water use, end uses, water treatment and cost of water in Canada for industrial users. The survey was done under the federal Statistics Act under an agreement between Statistics Canada and Environment Canada. The survey was mailed out to about 6,100 industrial establishments from four sectors: manufacturing, mineral extraction, thermal power, and hydro power. Their findings indicated that production of one kilowatt-hour of electricity requires 140 litres (36.99 gallons) of water for fossil fuel plants and 205 litres (54.16 gallons) for nuclear power plants. Some of the water is converted to the steam which drives the generator producing the electricity. Most of the water, however, is used for condenser cooling.

The utilization of Photovoltaics however, as a renewable energy resource, requires less than one gallon of water per kWh for both withdrawal and consumption (Energy Foundation, 2003). Water usage is primarily incidental for the cleaning of the panels. In regions such as the western United States experiencing a multi-year drought, water rights and water resource management have gained significant importance and attention by local and regional regulatory authorities.

7.0 DISCUSSION

This study was undertaken to evaluate sustainable mechanisms to mitigate the urban heat island hysteresis lag effect of surface pavements. The findings identified opportunities to utilize renewable energy sources to potentially mitigate urban heat island pockets (micro-scale) which can be expanded in a meso-scale model such as MM5 to evaluate at what scale of implementation the mitigation can serve to reduce the meso-scale urban heat island effect within a region. The research area of Phoenix, Arizona is experiencing its 7th straight year of drought conditions in an already arid region. Conventional urban forestry campaigns to mitigate the hysteresis lag effect will most certainly have an initial net increase in water use consumption within a region as plants try to establish and over come elevated rhizosphere temperatures. Conversely, the utilization of photovoltaics as a mitigation strategy can result in a reduction of water usage by minimizing the need for water intensive thermoelectric power generation sources to meet base energy needs as well as having the compounded benefit of potentially reducing mechanical cooling needs by reducing the hysteresis lag effect. Photovoltaics provide for an alternative source to meet the increasing peak energy demand in the Phoenix region and unlike urban forestry, the PV canopy coverage reaches maximum micro-scale attainment upon construction.

Further researcher is being undertaken to quantify the life cycle benefits of this renewable energy mitigation scheme by quantifying a regional energy and water balance and added opportunities that coupled techniques such as a combination of permeable pavement materials and renewable technologies (Figure #16) can provide for regions to meet the challenges of sustainability.

Increased reductions of engineered canopy temperatures will be modeled by computational fluid dynamics to identify optimal spacing between the upper layer of the metal canopy to the bottom of the photovoltaic panels. As bandgap technologies improve it will not only provide for a more beneficial cost-benefit based on upon solar cell efficiencies but can improve the thermodynamic balances as they relate to the urban heat island effect.

REFERENCES

Akbari, H., Betz, S.E., Hanford, J.W., Kurn, D.M., Fishman, B.L., Taha, H.A. and Bos, W. (1993) Monitoring Peak Power and Cooling Energy Savings of Shade Trees and White Surfaces in the Sacramento Municipal Utility District (SMUD) Service Area: Data Analysis, Simulations, and Results. Lawrence Berkeley Laboratory Report 34411, pp. 146.

Akbari, H., Rose, L. & Taha H. (1999). Characterizing the Fabric of the Urban Environment: A case study of Sacramento, California. Lawrence Berkeley National Laboratory, US Department of Energy. LBNL-44688.

Asaeda, T. Ca VT. & A. Wake. (1996). Heat storage of pavement and its effect on the lower atmosphere. Atmospheric Environment **30**: 413-427

Baker, Lawrence, A., Brazel, A.T., Westerfhoff, P. (2004). Environmental consequences of rapid urbanization in warm, arid lands: case study of Phoenix, Arizona (USA). Sustainable Cities 2004 – Sienna, Italy.

Brazel, A. & Quatrocchi, D. (2004). Urban Climatology. The Encyclopedia of World Climates. John E. Oliver (ed). Kluwer Academic Publishers.

Brazel, A. (2003). Future climate in central Arizona: Heat and the role of urbanization (Research Vignette No. 2). Tempe, AZ: Consortium for the Study of Rapidly Urbanizing Regions – Arizona State University.

Brown, M. J., and Grimmond, S. (2001). Sky View Factor Measurements in Downtown Salt Lake City-Data Report for the Urban DOE CBNP Urban Experiment. Los Alamos National Laboratory. LA-UR-01-1424

Carr, J.E., Chase, E.B., Paulson, R.W., and Moody, D.W., (1990). National water summary 1987--hydrologic events and water supply and use: U.S. Geological Survey Water-Supply Paper 2350, p. 467-474.

Celestian, S. & C. Martin. (2003). Leaf physiology of four landscape trees in response to commercial parking lot location. Central Arizona Phoenix – Long Term Ecological Research. NSF.

Chapman, L, Thornes JE and Bradley, AV (2001) Rapid determination of canyon geometry parameters for use in surface radiation budgets, *Theor. & App. Met.*, 69, 81-89

Crafts-Brandner, S.J. and Salvucci, M.E. (2000) Rubisco activase constrains the photosynthetic potential of leaves at high temperature and CO2. *Proc. National Academy of Sciences, USA* **97**, 13430–13435.

DeVoss, A (1992). Endoreversible thermodynamics of solar energy conversion. Oxford University Press. ISBN 0 - 19 - 851392 - 5

Energy Foundation (2003). The Last Straw-Water Use by Power Plants in the Arid West. In Association with the Hewlett Foundation a joint initiative of The John D. and Catherine T. MacArthur Foundation, The McKnight Foundation, The Joyce Mertz-Gilmore Foundation, The David and Lucile Packard Foundation and the Pew Charitable Trusts.

Farrar, J.F. and Williams, M.L. (1991). The effects of increased atmospheric carbon dioxide and temperature on carbon partitioning, source-sink relations and respiration. *Plant Cell and Environment* **14**, 819–830.

Genchi, Y., Ishisaki, M., Ohashi, Y., Takahashi, H. and A. Inaba (2003). Impacts of Large-Scale Photovoltaic Panel Installation on the Heat Island Effect in Tokyo. Fifth Conference on the Urban Climate

Golden, J. S. (2004). The Built Environment Induced Urban Heat Island Effect in Rapidly Urbanizing Arid Regions – A Sustainable Urban Engineering Complexity. Environmental Sciences – In Print.

Hansen, J.W., Hodges, A. W., & Jones, J.W., (1999). ENSO influences on agriculture in the southeastern US. *J. Climate*, 11, 404-411.

Huxman, T.E., Hamerlynck, E.P., Loik, M.E. and Smith, S.D. (1998) Gas exchange and chlorophyll fluorescence responses of three south-western *Yucca* species to elevated CO2 and high temperature. *Plant Cell and Environment* **21**, 1275–1283.

Jacoby, M. (2004). Photovoltaic Cells: Power at a Price. *Chemical and Engineering News*. June 21, 2004. Volume 82, Number 25 pp. 29-32 ISSN 0009-2347

Jordon, D.B. and Orgen,W.L. (1984) TheCO2/O2 specificity of ribulose 1,5-bisphosphate carboxylase/oxygenase. *Planta* **161**, 308–313.

Kjelgren R. & T. Montague. (1998). Urban tree transpiration over turf and asphalt surfaces. Atmospheric Environment **32**: 35-41

Law, R.D. and Crafts-Brandner, S.J. (1999) Inhibition and acclimation of photosynthesis to heat stress is closely correlated with activation of ribulose-1,5-bisphosphate carboxylase/oxygenase. *Plant Physiology* **120**, 173–181.

Martin, C.A. and Stabler, L.B. (2002) Plant gas exchange and water status in urban desert landscapes. *Journal of Arid Environments*, **51**, 235–254.

Martin, C.A., Stutz, J.C., Kimball, B.A., Idso, S.B. and Akey, D.H. (1995) Growth and topological changes of *Citrus limon* (L.) Burm. f. 'Eureka' in response to high temperatures and elevated atmospheric carbon dioxide.

McPherson, E.Gl, Simpson, J.R., Peper, P. & Xiao, Q. (1999). Benefit-Cost Analysis of Modesto's Municipal Urban Forest. Journal of Arboriculture, **25(5)**:235-248.

National Energy Technology Laboratory – U.S. Department of Energy (2004). Water and Energy: Addressing the Critical Link Between The Nation's Water Resources and Reliable and Secure Energy.

Oke, T.R., (1987). Boundary layer climates (2nd ed.). London: Routledge.

Oke, T.R., (1992). Boundary layer climates (2nd ed.). London: Routledge

Rokka, A., Aro, E.M., Herrmann, R.G., Andersson, B. and Vener, A.V. (2000) Dephosphorylation of photosystem II reaction center proteins in plant photosynthetic membranes as an immediate response to abrupt elevation oftemperature. *Plant Physiology* **123**, 1525–1535.

Salt River Project (2003). http://www.srpnet.com/environment/solarparking.asp

Scharf, D., Burke, D., Villeneuve, M., Leigh, L. (2002). Industrial Water Use 1996. Environmental Economics Branch, Environment Canada. Minister of Public Works and Government Services Canada. Catalogue No. En40-669/2002E
ISBN 0-662-32682-2

Scott, K.I., Simpson, J.R., and E.G. McPherson. 1999. Effects of tree cover on parking lot microclimate and vehicle emissions. Journal of Arboriculture 25(3): 129-142. Online at http://wcufre.ucdavis.edu/effects_of_tree_cover_on_parking.htm

Southwest Energy Efficiency Project - SWEEP (2002). The New Mother Lode. The Potential for More Efficient Electricity Use in the Southwest. Energy Foundation. In Association with the Hewlett Foundation a joint initiative of The John D. and Catherine T. MacArthur Foundation, The McKnight Foundation, The Joyce Mertz-Gilmore Foundation, The David and Lucile Packard Foundation and the Pew Charitable Trusts.

U.S. Department of Agriculture, National Agricultural Statistics Service, 1999, Ranking of States and Counties: 1997 Census of Agriculture, vol. 2, subject series p.

2, 110 p., accessed December 18, 2003, at
http://www.nass.usda.gov/census/census97/rankings/rankings.htm

U.S. Department of Agriculture, National Agricultural Statistics Service, 2000, Drought and Fire Survey 2000, Montana's 2000 Drought/Fire Survey Results: press release, accessed June 25, 2003, at
http://www.nass.usda.gov/mt/pressrls/misc/firesurv.htm

USGS (2004). Estimated Use of Water in the United States in 2000. Contributors Hutson, S., Barber, N., Kenny, J., Linsey, K., Lumia, D., and Molly A. Maupin. USGS Circular 1268, 15 figures, 14 tables (released March 2004, revised April 2004, May 2004**)**

Van Iersel, M.W. and Linstrom, O.M. (1999) Temperature response of whole plant CO2 exchange rates of three magnolia cultivars. *J. American Society for Horticultural Science* **124**, 277–282.

Xiao X, Melillo JM, Kicklighter DW, McGuire AD, Prinn RG, Wang C, Stone PH, Sokolov A (1998) Transient climate change and net ecosystem production of the terrestrial biosphere. *Global Biogeochemical Cycles* **12,** 345-360.

Yu, K.M., Walukiewicz, W., Wu, J., Shan,W., Beeman, J., Scarpulla, M., Dubon, O. and Becla, P. (2003). Dilluted II-VI Oxide Semiconductors with Multiple Band Gaps. American Physical Society. Volume 91, Number 24.

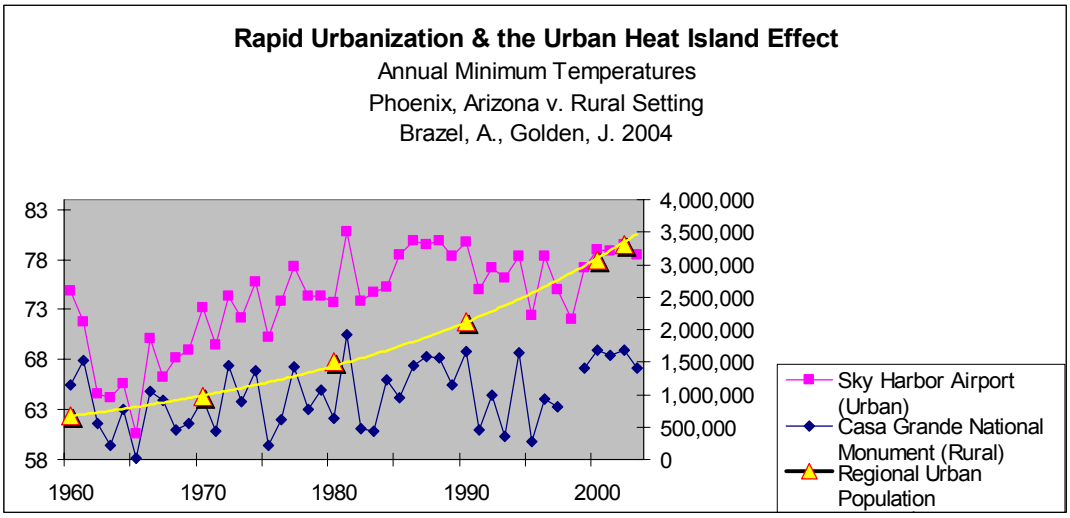

Graph #1. The Urban Heat Island Effect of the Phoenix, Arizona Region. Increased urban population as it correlates to annual minimum temperatures as compared to an un-disturbed rural setting.

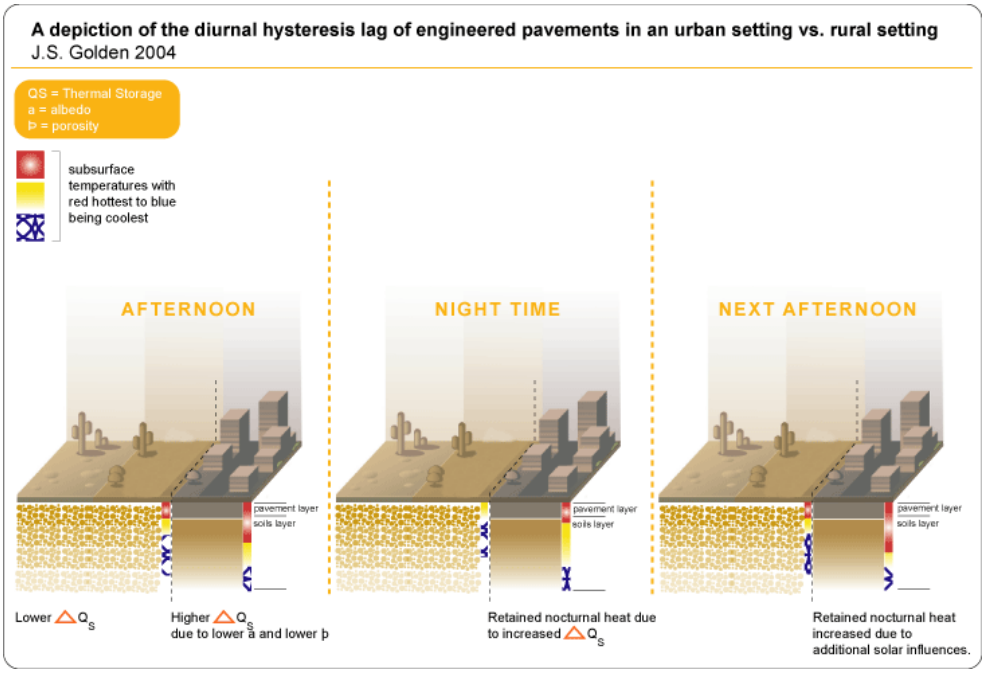

Figure #1. A representation of the urban heat island induced surface pavement hysteresis lag effect.

Figure 2. *Controlled parking lot utilized for research of urban forestry mitigation*.

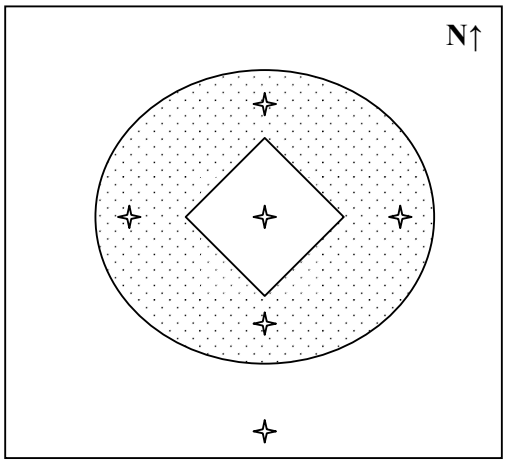

Figure 3. *Urban forestry sampling plan.*

✧ *= thermocouples.*

Shading = canopy coverage
** not to scale.*

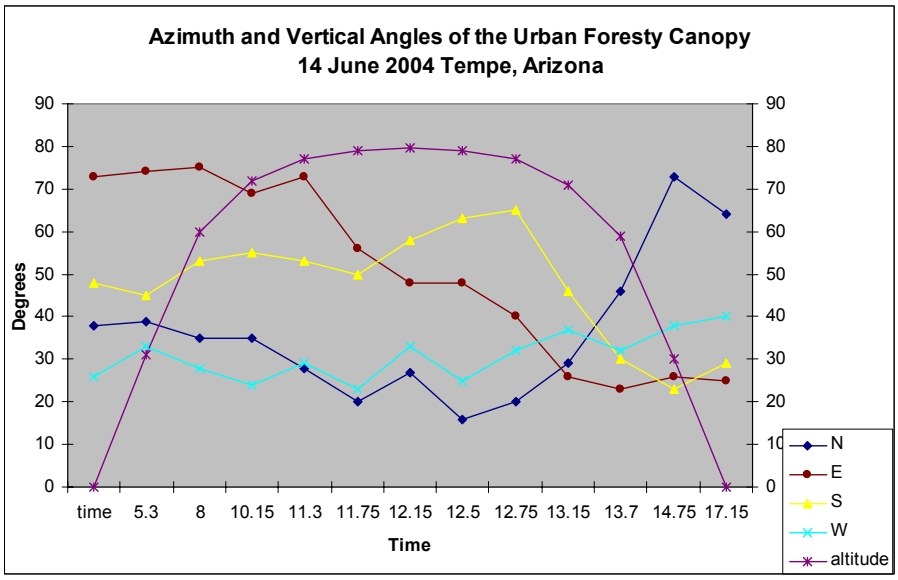

Figure #4: *Sky View Factor and Temperature Response.*

Figure #5. *Sky-view factor as documented with fish-eye lens.*

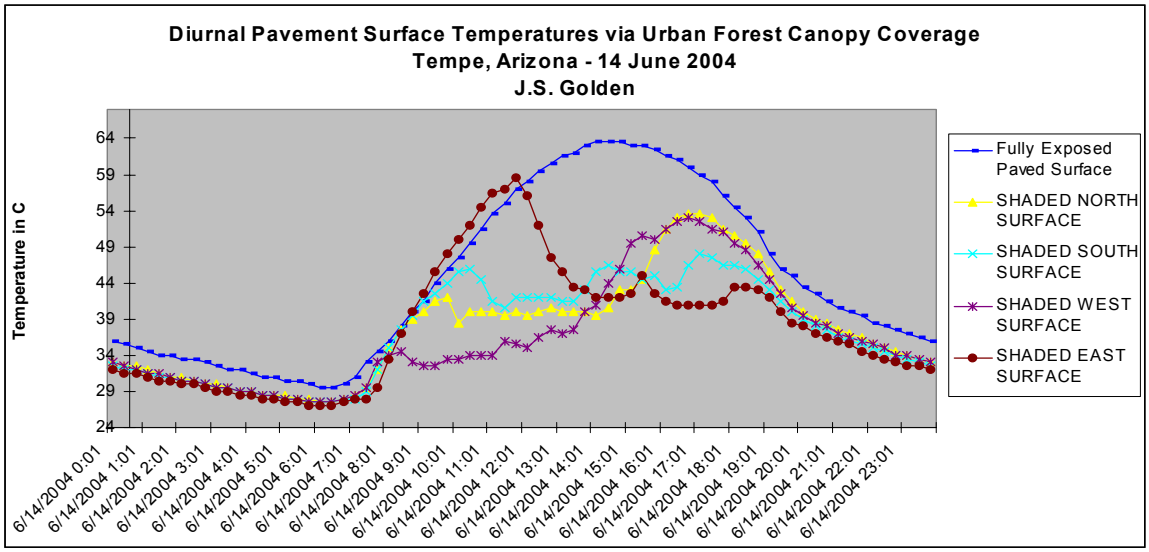

Figure #6. *Reaction of surface pavement temperatures as a function of sky view factor.*

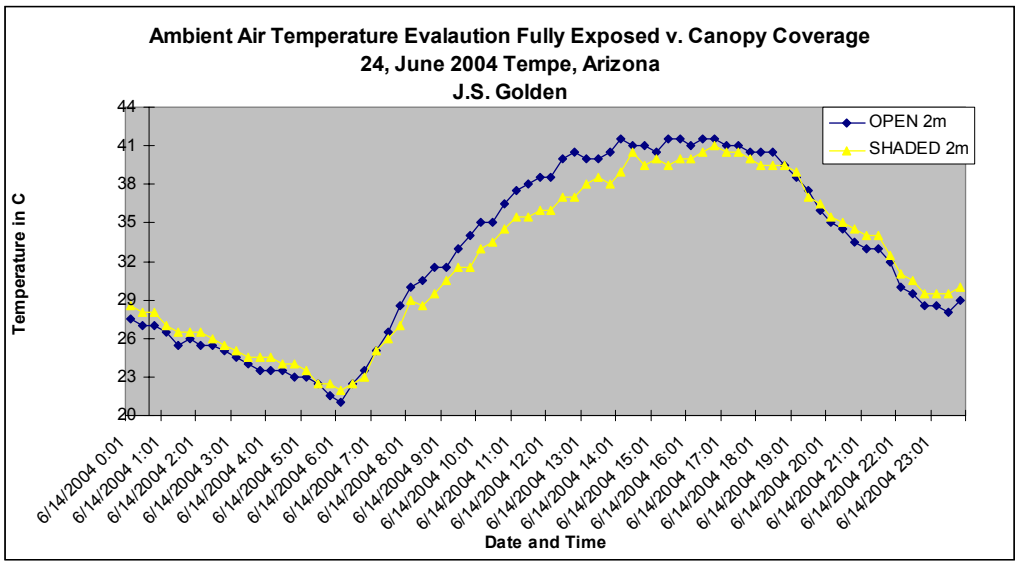

Figure 7*. Human Comfort as a function of ambient temperature.*

Figure #8. *Subject research site for PV canopy coverage.*

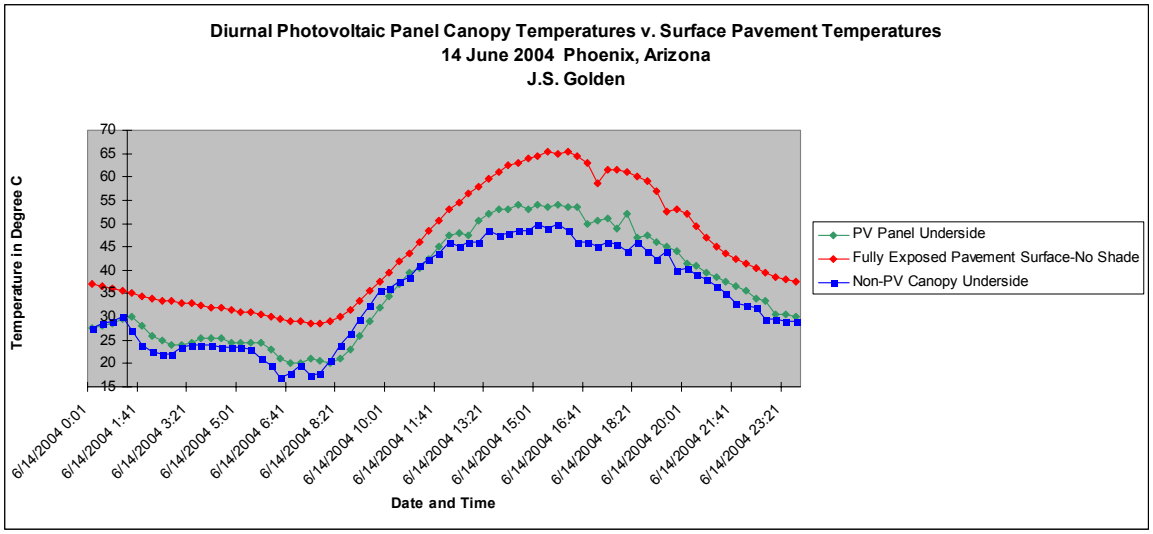

Figure #9. *Diurnal variance of surface temperatures utilizing PV canopy coverage.*

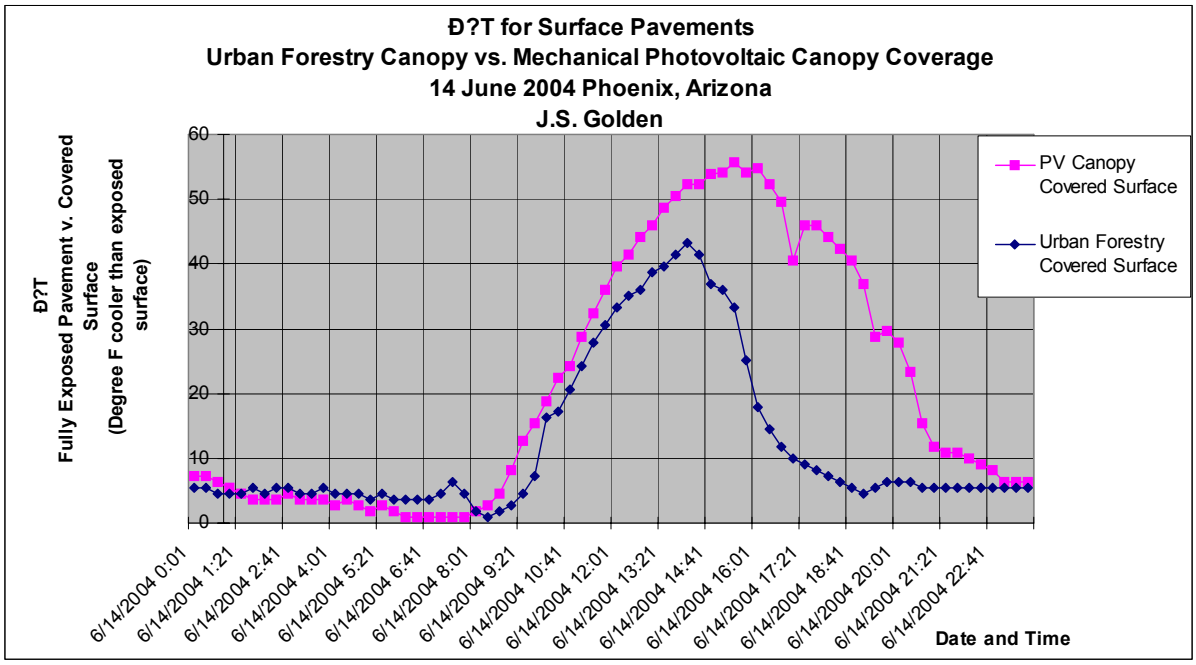

Figure #10. *Graph of the surface pavement mitigation benefits between PV Canopy coverage and Urban Forestry Coverage.*

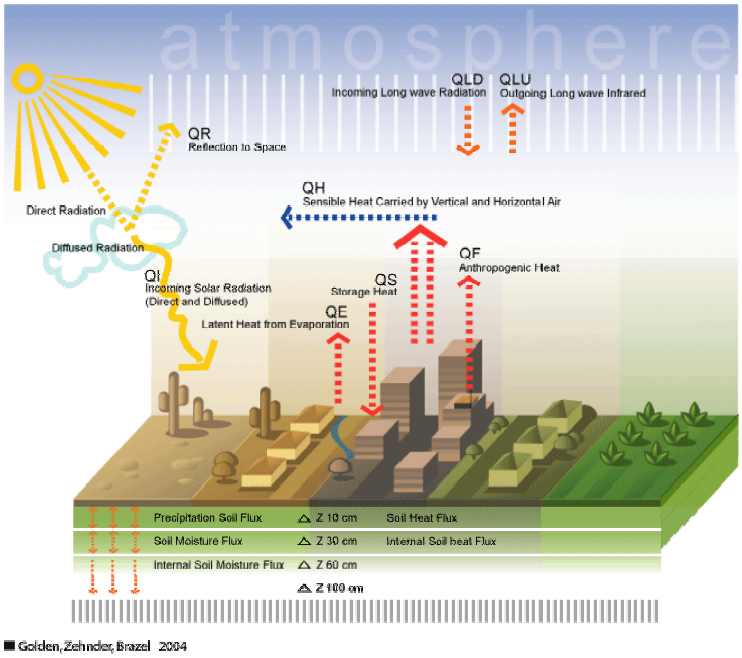

Figure #11. *The Atmospheric Physics Representation. Golden (2004).*

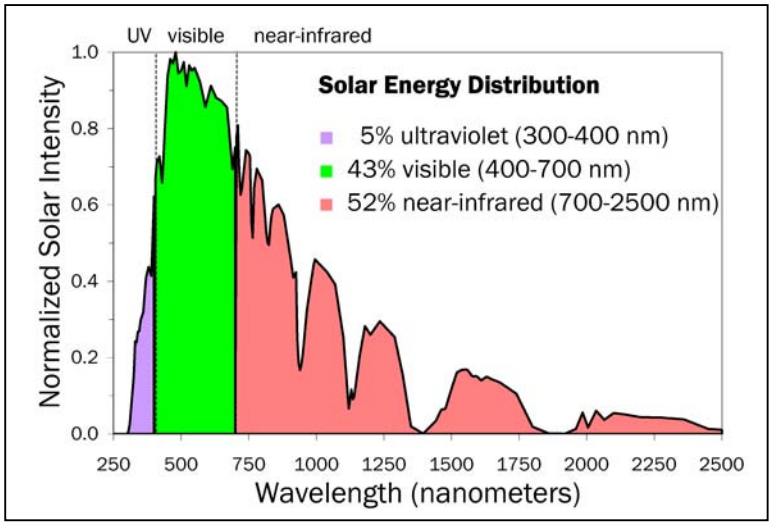

Figure #12: Solar Energy Distribution. Lawrence Berkeley National Laboratory.

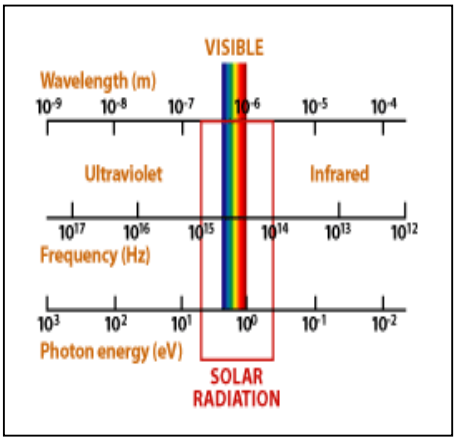

Figure #13: Solar Radiation Wavelengths. Source: NASA.

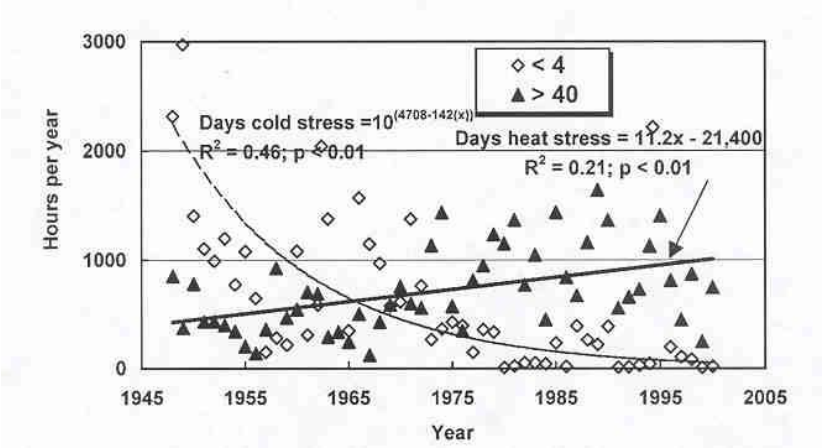

Figure #14 Hours of plant cold stress and heat stress per year at Sky Harbor, 1948-2000. Baker et al. 2003.

Figure 15. *Total United States water withdrawals by category, 2000. Source: U.S.G.S. 2000*

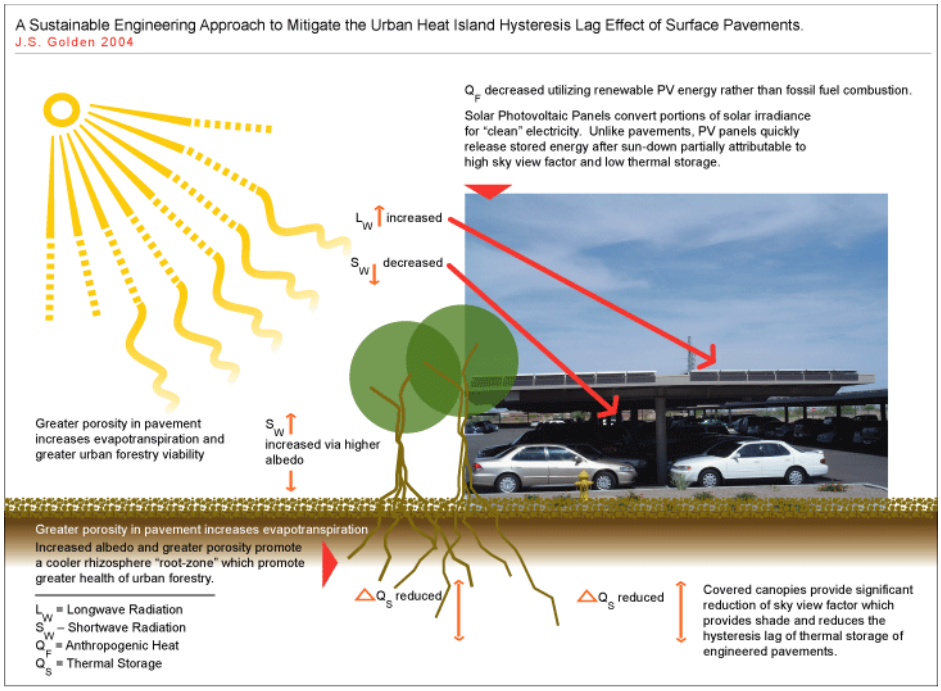

Figure #16. Sustainable Engineering Approaches to Mitigating Surface Pavement Hysteresis Lag Effect in Parking Lots.